Student thesis series INES nr 329

Modeling the potential impact of climate change on the distribution of Western Corn Rootworm in Europe

Tetiana Svystun

2015

Department of

Physical Geography and Ecosystems Science

Lund University

Sölvegatan 12

Tetiana Svystun (2015). *Modeling the potential impact of climate change on the distribution of Western Corn Rootworm in Europe*
Master degree thesis, 30 credits in *Physical Geography and Ecosystem Analysis*
Department of Physical Geography and Ecosystems Science, Lund University

Level: Master of Science (MSc)

Course duration: *September* 2014 until *January* 2015

Disclaimer

Modeling the potential impact of climate change on the distribution of Western Corn Rootworm in Europe

Tetiana Svystun

Master thesis, 30 credits, in *Physical Geography and Ecosystem Analysis*

Supervisor Anna Maria Jönsson
Department of Physical Geography and Ecosystem Science
Lund University, Sweden

Exam committee:
Paul Miller, Department of Physical Geography and Ecosystem Science, Lund University
Cecilia Akselsson, Department of Physical Geography and Ecosystem Science, Lund University

Acknowledgment

I am grateful to my supervisor Anna Maria Jönsson for her constant support, inspiration and patience during the entire working process.

I acknowledge the E-OBS dataset from the EU-FP6 project ENSEMBLES (http://ensembles-eu.metoffice.com) and the data providers in the ECA&D project (http://www.ecad.eu).

I acknowledge the World Climate Research Programme's Working Group on Regional Climate, and the Working Group on Coupled Modelling, former coordinating body of CORDEX and responsible panel for CMIP5. I also thank the climate modelling groups of Danish Meteorological Institute, Royal Netherlands Meteorological Institute and Rossby Centre in Swedish Meteorological and Hydrological Institute for producing and making available their model output. I also acknowledge the Earth System Grid Federation infrastructure an international effort led by the U.S. Department of Energy's Program for Climate Model Diagnosis and Intercomparison, the European Network for Earth System Modelling and other partners in the Global Organisation for Earth System Science Portals (GO-ESSP).

Abstract

The Western Corn Rootworm (WCR), *Diabrotica virgifera virgifera*, is an important insect pest of maize, which has been introduced into Europe from Northern America in 1980s. Since then, its distributional range is continuously expanding over the Central and South-Eastern Europe. This study assessed the potential effect of increased temperatures on the timing of WCR generation development and on the WCR distributional range in 2011-2100. An impact model, describing a linear relationship between temperature and thermal requirements for the complete development of adult WCR, was forced by an ensemble of climate model data from three regional climate models, representing two different future scenarios. The impact model simulations showed the fulfillment of temperature requirements in earlier date and over the extended area, covering continental Europe, large parts of British Isles and Scandinavia, in 2011-2100 in comparison with 1981-2005. In addition, the impact model projections display an increase in frequencies of years in which the temperature requirements of the WCR are fulfilled, thereby indicating a future northward extension of area suitable for the establishment of a permanent WCR population.

Table of Contents

Abbreviations

WCR – Western Corn Rootworm

SET – sum of effective temperatures

DD – degree days

EPPO – European and Mediterranean Plant Protection Organization

GCM – global climate model

RCM – regional climate model

RCP – Representative Concentration Pathway

CMIP – Coupled Model Intercomparison Project Phase 5

WCRP – World Climate Research Programme

CORDEX – Coordinated Regional Downscaling Experiment

SMHI – Swedish Meteorological and Hydrological Institute

DMI – Danish Meteorological Institute

KNMI – Royal Netherlands Meteorological Institute

NE – Northeastern Europe

SC – Scandinavia

BI – British Isles

FR – France

ME – Mid-Europe

EE – Eastern Europe

MD – Mediterranean

IP – Iberian Peninsula

AL – Alps

1 Introduction

There is a complex interaction between environment, host plant and insect pest within an agro-ecosystem, which may be altered by climate change, affecting agricultural production (Newton et al. 2011, Fand et al. 2012). Understanding the potential responses of these interactive components to climate change may help to develop relevant approaches in agricultural pest management with implications for a food security (Gordh and McKirdy 2013). In this regard, assessment of climate change impact on insect pests is of great importance, since insects serve as yield-determining agents and as early indicators of environmental fluctuations (Scherm et al. 2000). A range of climate data, produced by regional climate models through downscaling of global climate scenarios, allows to perform such analysis on the regional scale (Jacob et al. 2014).

This study will focus on the Western Corn Rootworm (WCR), *Diabrotica virgifera virgifera*, an important insect pest of maize, which significantly reduces yield by damaging maize roots (Meinke et al. 2009). The WCR has been recognized as a major maize pest in North America, but it can become equally important in Europe, as it was accidentally introduced from North America into Europe with air traffic and detected for the first time near Belgrade airport, Serbia, in 1992. Since then, its distributional range has been expanding northward, from Southern and South-Eastern into Central Europe, currently reaching southern Poland (Meinke et al. 2009, Wilstermann and Vidal 2013).

The WCR development is temperature-dependent, therefore a future climate plays an important role in the risk of WCR establishment in different European regions. In other words, the future temperature conditions at the higher latitudes may allow the WCR to complete its life cycle and found new populations. The WCR thermal constants (amount of thermal energy needed for initiating and completing the different life stages) can be used to determine the specie occurrence under projected temperature regimes (Wilstermann and Vidal 2013).

The aim of this study is to analyze the potential effect of climate change on the timing of WCR generation development, thereby to investigate, which parts of Europe will be suitable for the WCR population establishment under projected climatic conditions of the 21st century. In this respect, the experimentally determined thermal requirements (Streda et al. 2013) for the complete development of adult individual will be used for creation of an impact model, which will be further forced by an ensemble of climate model data, representing two different future scenarios.

The hypothesis is that climate change and associated temperature increase will allow a northward expansion of the WCR distributional range in Europe.

2 Background

2.1 Effects of temperature on insect pests

The impact of climatic parameters, notably temperature, on insect pests can be direct, affecting their development, reproduction, survival, behavior, distribution, migration and adaptation. Moreover, an indirect influence can occur through the effects of climate on the host plant, interacting species, natural enemies and competitors (Porter et al. 1991).

In the context of the current study, the effects of temperature on insect pest life cycle are of the main interest. The development of insects, as poikilothermic organisms (whose body temperature varies with the surrounding temperature), is temperature-dependent, occurring within particular temperature ranges, the lower and upper developmental thresholds. Two essential constants for the prediction of specific life cycle events, life stages, can be defined from the relationship between the duration of development and temperature: (i) the lower developmental threshold and (ii) the thermal constant (an amount of thermal energy required to complete developmental process), which is based on the sum of effective temperatures (SET) (temperatures above the lower developmental threshold) and expressed as degree days (DD) (Trudgill et al. 2005).

In addition, the life cycle of many insects is synchronized with the phenology of the host plant, which also depends on temperature. Thereby, a temperature, by affecting development and availability of both insect pest and host plant, determines the lower and upper limits of the insect distributional range (Bale et al. 2002).

The temperature rise, associated with climate change, may have the following consequences for insect: faster time of the development, increased number of generations per year for multivoltine species (complete several generations per year), changes in population size and density, longer period suitable for the development, alteration of the synchrony with the host plant, increased overwintering survival, extension of the distributional range to higher latitudes and altitudes, and introduction of alternative or temporary hosts (Porter et al. 1991, Bale et al. 2002).

2.2 WCR life cycle

The WCR is a univoltine specie (completes one generation per year), and its development goes through four life stages: (a) egg, (b) larvae, (c) pupa and (d) adult. The attainment and duration of each stage depend on temperature, therefore varying between the different climatic regions (Hemerik et al. 2004, Meinke et al. 2009). The main features of the WCR life cycle in the temperate regions are presented in Figure 1 and described below.

a) The eggs deposition occurs in the soil during July-September, following by the winter dormancy, diapause. The postdiapause development requires soil temperature above 11°C and water uptake (Wilde 1971).
b) The eggs hatch usually takes place in late May or in early June. The larval development passes through three stages, instars, under the following lower developmental thresholds: 10.5°C and 9.8°C for the first male and female instars, respectively; 9.6°C and 5.5°C for the second male and female instars, respectively; 8.3°C and 7.8°C for the third male and female instars, respectively (Jackson and Elliot 1988).
c) The third larval stage pupates in the soil above the temperature of 9.7°C (Jackson and Elliot 1988).
d) The pupa completes development, having the lower and upper developmental thresholds near 9°C and 30°C, respectively. The emergence of adults commonly starts in late June or early July. Soon after they mate, and the females start ovipositing in two weeks after mating (Hemerik et al. 2004, Meinke et al. 2009). The adults remain in the field until the first frost (Sivčev et al. 2012).

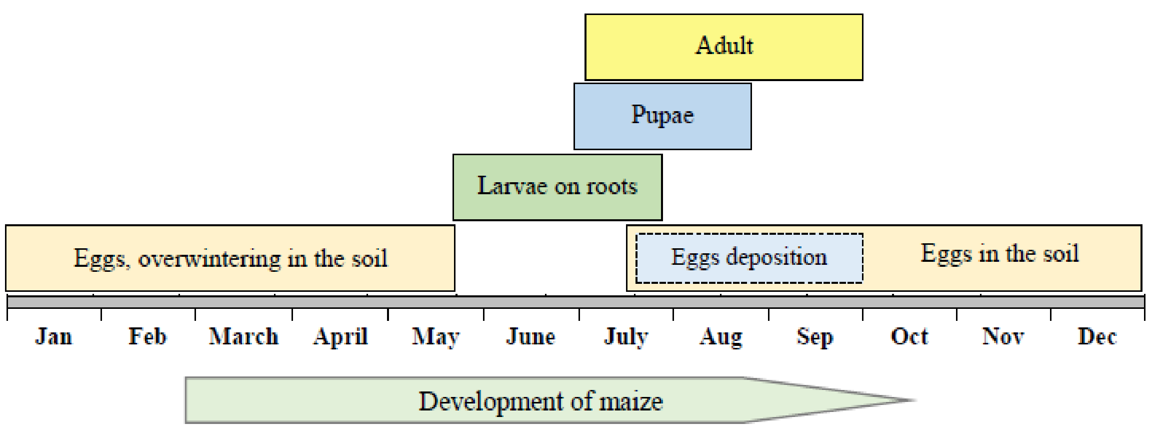

Figure 1 *Schematic representation of the WCR life cycle in the temperate regions.*

2.3 Damage by WCR to maize plant

The WCR cause damage to maize both as larvae and as adults. The first larval stage reaches a root and starts feeding on the fine root hair. As growing and requiring more food, larvae burrows into the root tips and channels upwards to reach the plant base. The latter larval stages feed on larger primary roots (Chiang 1973). The larval feeding on maize root system causes root injury, decreasing the plant uptake of water and nutrients, thereby reducing plant growth and yield (Hemerik et al. 2004). More severe root damage may lead to the plant falling, making it difficult to be harvested, and resulting in additional yield losses (Lammers 2006). Reported maize yield reduction varies within the range of 10-40% (Wesseler and Fall 2010).

The WCR adults feed on the different parts of maize plant: leaves, pollen, silks and young kernels. By feeding on leaves, they remove the epidermis and chew holes on the leaf tissue, but this is not considered as an important damage. Significant damage may occur if the adults feed on the fresh silks before or during the pollination process, resulting in poorly filled ears and loss of seeds quality and quantity. This is however rather uncommon (Lammers 2006).

2.4 WCR distribution in Europe

The first outbreak of the WCR in Europe was observed in the maize field near Belgrade airport, Serbia, in 1992. It is assumed that the WCR was introduced from the Midwestern United States (north-central states of the United States of America) by intercontinental flights 8-13 years prior to the first detection (Meinke et al. 2009, Szalai et al. 2011). The first introduction was followed by several others in different parts of Europe through the traffic by air, road and water. Once established, the WCR started spreading with the average annual rate of 40 km. The area of the WCR distribution is continuously expanding over the Central and South-Eastern Europe (Lammers 2006, Meinke et al. 2009). However, the factors, such as topographical features (mountains and large water bodies), and temperatures at northern latitudes and higher altitudes, may influence the rate and direction of spread (Meinke et al. 2009).

According to the European and Mediterranean Plant Protection Organization (EPPO) (URL: https://gd.eppo.int/taxon/DIABVI/distribution), currently, the WCR is widespread in Hungary, Romania and Slovakia; restricted in Albania, Austria, Bosnia and Hercegovina, Bulgaria and Croatia, Check Republic, France, Greece, Italy, Poland, Serbia and Ukraine; under eradication in Belgium, Germany and Switzerland; and few specimens have been observed in Belarus, Slovenia and United Kingdom.

2.5 Overview of climate modeling and impact modeling

The climate system has been instrumentally observing since the mid-19th century, providing evidence of the climate change. In order to understand current and future climate responses to natural and anthropogenic influences, the climate models of different complexity are used, depending on the scientific question being addressed (IPCC 2013).

Global climate models (GCMs) operate at a coarse spatial resolution of a few hundred kilometers (at best around 100-200 km) (Rummukainen 2010), representing the dynamics of physical components of climate system (Atmosphere–Ocean General Circulation models), which may be coupled to the biogeochemical cycles (Earth System models). GCMs may be forced either by emissions or concentrations of greenhouse gases, which are specified according to the scenario (IPCC 2013). The latest GCM simulations have been performed under the framework of the Coupled Model Intercomparison Project Phase 5 (CMIP5) of the World Climate Research Programme (WCRP), using a new set of forcing scenarios, the Representative Concentration Pathways (RCPs) (Taylor et al. 2012). There are four different RCPs, namely RCP2.6, RCP4.5, RCP6.0 and RCP8.5, which are identified by possible radiative forcing value at the end of the 21st century. Each RCP assumes a trajectory to a particular target radiative forcing by means of providing the input variables (e.g. emissions and concentrations of greenhouse gases, short-lived gases and aerosols, land use/cover changes, etc.) for GCM simulations needed to reach that target (Moss et al. 2010, IPCC 2013).

Regional climate models (RCMs) describe climate processes at a finer spatial resolution than the GCMs (12.5-50 km) (Jacob et al. 2014), and they can be used for dynamic downscaling of output for a particular geographical region (IPCC 2013). In this regard, lateral (vertical profiles of temperature, moisture and wind) and often surface (sea surface temperature, sea ice and pressure) boundary conditions (with temporal resolution typically of 6 hours) from GCM are applied along the edges and surface of the regional domain; and the atmospheric circulation together with surface interactions inside the domain are reproduced by the RCM (Rummukainen 2010, Hostetler et al. 2011).

RCMs projections provide data for a variety of applications, including assessments of the climate change impact (Rummukainen 2010). State-of-the-art generation of regional climate projections is given in the frame of the WCRP Coordinated Regional Downscaling Experiment (CORDEX), applying the most recent versions of RCMs with the lateral boundary conditions from CMIP5 GCM simulations (Jacob et al. 2014).

The performance of impact models, driven by climate model data, is influenced by various sorts of uncertainties, introduced at different stages of the modeling process. The following major sources of uncertainties are identified: uncertainties related to observation data, uncertainties associated with forcing scenario, global model uncertainty (the choice of boundary conditions for driving RCM) due to the different responses of the large-scale dynamics, regional model uncertainty (the choice of RCM data for driving impact model) due to the different techniques for representing small-scale physics and dynamics, and modeling uncertainty inherent in the model construction and parameterisation. One of the ways to account for uncertainties associated with regional and global climate simulations is to use a group of data, ensemble, from several climate models (Déqué et al. 2012).

3 Material and Methods

3.1 WCR model

In this study, an impact model, depicting quantitative relationship between thermal conditions and development of adult WCR, which corresponds to completed development of WCR generation, was created in Matlab software (version R2014a) to analyze the potential effect of climate change on the WCR development. Impact model was denoted as the WCR model.

The WCR thermal constants have been determined by Streda et al. (2013) in the course of the field experiment, evaluating the temperatures of 10°C (at 0.05 m above the ground) and 12.5°C (at 2 m above the ground) as lower developmental thresholds. Considering the results of abovementioned field experiment as the most recent and availability of climate data (daily mean temperature at 2 m above the ground), two temperature requirements for the development of adult WCR were used for the WCR model parameterisation: (I) a lower developmental threshold of +12.5°C and (II) SET at 2 m above the ground of 415 DD. The day of the year which fulfills temperature requirements was computed for each grid cell (referring to the spatial resolution of the climate data) in the following way.

Firstly, the effective daily mean temperature ($T_i^{effective}$) was calculated as:

$$T_i^{effective} = \begin{cases} T_i - T_{threshold}, & T_i > T_{threshold} \\ 0, & T_i \leq T_{threshold} \end{cases} \quad \textbf{(1)}$$

where T_i is a daily mean temperature at 2m above the ground for day i of the year and $T_{threshold}$ is a lower developmental threshold.

Secondly, the SET for each day of the year (DD_i) was computed starting from the first day of the year to the day i:

$$DD_i = \sum_{j=1}^{i} T_j^{effective} \quad \textbf{(2)}$$

Finally, the day of the year which fulfills temperature requirements is the first index k such that:

$$DD_k \geq DD_{threshold} \quad \textbf{(3)}$$

where $DD_{threshold}$ is a SET required for the emergence of adult individual.

3.2 Climate data sets

Daily mean temperature at 2m above the ground from two different climate data sets was applied as an input to the WCR model, both covering European domain and having the same spatial resolution of about 50×50 km (0.44×0.44^{o} rotated pole grid).

The first data set, the E-Obs (version 10), contains gridded observational data developed as a part of the European Union Framework 6 ENSEMBLES project (URL: http://ensembles-eu.metoffice.com) and provided by European Climate Assessment and Dataset (URL: http://www.ecad.eu) (Haylock et al. 2008). The E-Obs, spanning the period of 1981-2005, hereafter denoted as reference period, was used for validation of the impact model performance.

The second data set consists of an ensemble of data (Table 1) from three RCMs developed by the different institutions within CORDEX framework and is accessible via the CORDEX climate data node (URL: http://esg-dn1.nsc.liu.se/esgf-web-fe/). All three RCMs, namely RCA4 (Samuelsson et al. 2011), HIRHAM5 (Bøssing Christensen et al. 2007) and RACMO22E (Meijgaard et al. 2008), had been driven by lateral boundary conditions from global climate system model EC-EARTH (Hazeleger et al. 2010), employing historical and future forcing scenarios. The historical run is based on the observed concentration of greenhouse gases for the period of 1981-2005, while the future runs include natural and anthropogenic forcings according to the RCP4.5 and RCP8.5 for the period of 2011-2100. Both RCPs have similar radiative forcing magnitude and trend until 2035, resulting in minor differences in projected temperature. Later on, RCP's radiative forcing trajectory becomes more specific, i.e. RCP4.5 stabilizes radiative forcing at approximately 4.5 W/m^2 by the year 2100 on a pathway without overshoot, whereas RCP8.5 has continuous rising pathway reaching about 8.5 W/m^2 in 2100. Consequently, differences in projected temperature get more pronounced between the forcing scenarios during the second half of the 21st century (Moss et al. 2010). The data from future runs was divided into three time slices: 2011-2040, 2041-2070 and 2071-2100.

Table 1 List of input modelled climate time series and resulting impact model runs

Climate model data time series	Institute	Impact model run
tas_EUR-44_ICHEC-EC-EARTH_historical_r12i1p1_SMHI-RCA4_v1_day_1981-2005 tas_EUR-44_ICHEC-EC-EARTH_rcp45_r12i1p1_SMHI-RCA4_v1_day_2011-2040 tas_EUR-44_ICHEC-EC-EARTH_rcp45_r12i1p1_SMHI-RCA4_v1_day_2041-2070 tas_EUR-44_ICHEC-EC-EARTH_rcp45_r12i1p1_SMHI-RCA4_v1_day_2071-2100 tas_EUR-44_ICHEC-EC-EARTH_rcp85_r12i1p1_SMHI-RCA4_v1_day_2011-2040 tas_EUR-44_ICHEC-EC-EARTH_rcp85_r12i1p1_SMHI-RCA4_v1_day_2041-2070 tas_EUR-44_ICHEC-EC-EARTH_rcp85_r12i1p1_SMHI-RCA4_v1_day_2071-2100	Swedish Meteorological and Hydrological Institute (SMHI)	WCR_SMHI
tas_EUR-44_ICHEC-EC-EARTH_historical_r3i1p1_DMI-HIRHAM5_v1_day_1981-2005 tas_EUR-44_ICHEC-EC-EARTH_rcp45_r3i1p1_DMI-HIRHAM5_v1_day_2011-2040 tas_EUR-44_ICHEC-EC-EARTH_rcp45_r3i1p1_DMI-HIRHAM5_v1_day_2041-2070 tas_EUR-44_ICHEC-EC-EARTH_rcp45_r3i1p1_DMI-HIRHAM5_v1_day_2071-2100 tas_EUR-44_ICHEC-EC-EARTH_rcp85_r3i1p1_DMI-HIRHAM5_v1_day_2011-2040 tas_EUR-44_ICHEC-EC-EARTH_rcp85_r3i1p1_DMI-HIRHAM5_v1_day_2041-2070 tas_EUR-44_ICHEC-EC-EARTH_rcp85_r3i1p1_DMI-HIRHAM5_v1_day_2071-2100	Danish Meteorological Institute (DMI)	WCR_DMI
tas_EUR-44_ICHEC-EC-EARTH_historical_r1i1p1_KNMI-RACMO22E_v1_day_1981-2005 tas_EUR-44_ICHEC-EC-EARTH_rcp45_r1i1p1_KNMI-RACMO22E_v1_day_2011-2040 tas_EUR-44_ICHEC-EC-EARTH_rcp45_r1i1p1_KNMI-RACMO22E_v1_day_2041-2070 tas_EUR-44_ICHEC-EC-EARTH_rcp45_r1i1p1_KNMI-RACMO22E_v1_day_2071-2100 tas_EUR-44_ICHEC-EC-EARTH_rcp85_r1i1p1_KNMI-RACMO22E_v1_day_2011-2040 tas_EUR-44_ICHEC-EC-EARTH_rcp85_r1i1p1_KNMI-RACMO22E_v1_day_2041-2070 tas_EUR-44_ICHEC-EC-EARTH_rcp85_r1i1p1_KNMI-RACMO22E_v1_day_2071-2100	Royal Netherlands Meteorological Institute (KNMI)	WCR_KNMI

3.3 Analysis of the WCR model performance

The WCR model was driven by the E-Obs data set and by every modelled climate time series specified in Table 1. The resulting sets of the WCR model simulations were denoted as WCR_E-Obs, WCR_SMHI, WCR_DMI and WCR_KNMI (Table 1). An ensemble average of the climate model data was computed as a mean of (WCR_SMHI + WCR_DMI + WCR_KNMI), ignoring not numerical values, and denoted as WCR_Average. The results of the WCR model runs, that are day of the year and percentage of years when the temperature requirements for complete development of adult individual are fulfilled, were analyzed for the reference and future periods.

In order to assess the biases inherent in climate model data, the output from each individual ensemble members and ensemble average for the reference period was compared to the output from the WCR_E-Obs.

The spatial and interannual variability of the WCR model performance was captured by dividing the European domain into nine climatically comparable regions (Fig. 2) and comparing the results of the different model runs within and between regions. The regions are: Northeastern Europe (NE), Scandinavia (SC), British Isles (BI), France (FR), Mid-Europe (ME), Eastern Europe (EE), Mediterranean (MD), Iberian Peninsula (IP) and Alps (AL). They were defined based on the PRUDENCE project regions classification (Christensen and Christensen 2007), but with a slight modification to fit the current study, i.e. EE and MD were extended to the eastern border of the domain and NE was added. Also, the AL region was excluded from further analysis of the results due to the lack of generated numerical values for it.

The climate change signal was detected by comparing output from the WCR_Average for the future periods with the WCR_Average output for the reference period.

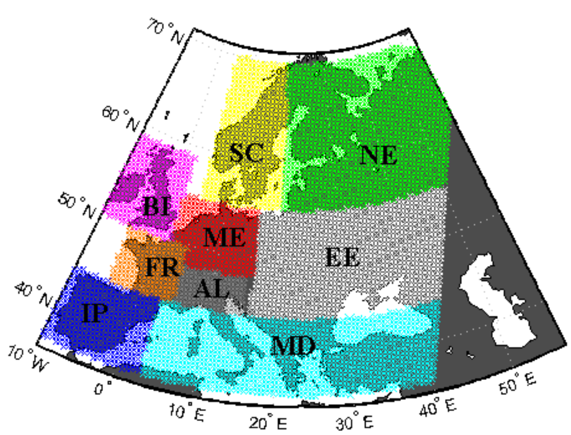

Figure 2 *Location of the regions used in the analysis of the impact model performance.*

4 Results

4.1 WCR model performance during reference period

4.1.1 Spatial patterns of the WCR model performance

An overview of spatial patterns of the WCR model performance within and between the different runs during the reference period is provided in Figure 3. A comparison between the impact model simulations using climate model data and observational data set indicates an ability of all ensemble members to capture a latitudinal gradient in timing and frequency of years of completed development of WCR generation.

The modelled time of the year for fulfilment of the temperature requirements (Eq. 3) is generally overestimated over a major part of Europe (Fig. 3A and 3B). However, the bias magnitude varies spatially among individual ensemble members. Thus, the greatest delay in timing for the WCR_SMHI is up to one month in Eastern Europe, France and in the north of Iberian Peninsula. The WCR_DMI represents spatial variability in a similar way as the WCR_SMHI, but discrepancies are reduced over the entire Europe. The WCR_KNMI results in a significant overestimation of timing of about a month in France and partly in the southern regions, while lower overestimation occurs in the rest of analysed area.

A common feature to all the WCR model simulations driven by climate model data is an underestimation of the northward extension of the territory that supports development of WCR generation (Fig. 3A). This is more pronounced for the WCR_SMHI and WCR_DMI, as these runs do not generate numerical values for large parts of Scandinavia and northeastern Europe, whereas the WCR_KNMI provides such values at least for the northeastern Europe except Finland. Thus, the numerical values in the ensemble average for the northeastern Europe primarily originate from the WCR_KNMI.

The WCR_Average smoothes performance of the individual ensemble members leading to better correspondence with the WCR_E-Obs (Fig. 3A and 3B). Although the ensemble average provides more spatially homogenous pattern of difference from the WCR_E-Obs than any single impact model simulation, the abovementioned pattern is still diverse.

A comparison of frequency of years in which the temperature requirements for the development of adult WCR are fulfilled, produced by forcing the WCR model with different climate data sets (Fig. 3C), shows an agreement between all ensemble members and the WCR_E-Obs for the area south of 50^{o}N, which meets the temperature requirements during all years. On the other hand, there is an underestimation of the northward extension of frequency of years at latitudes between 50-60^{o}N by all impact model simulations using climate model data.

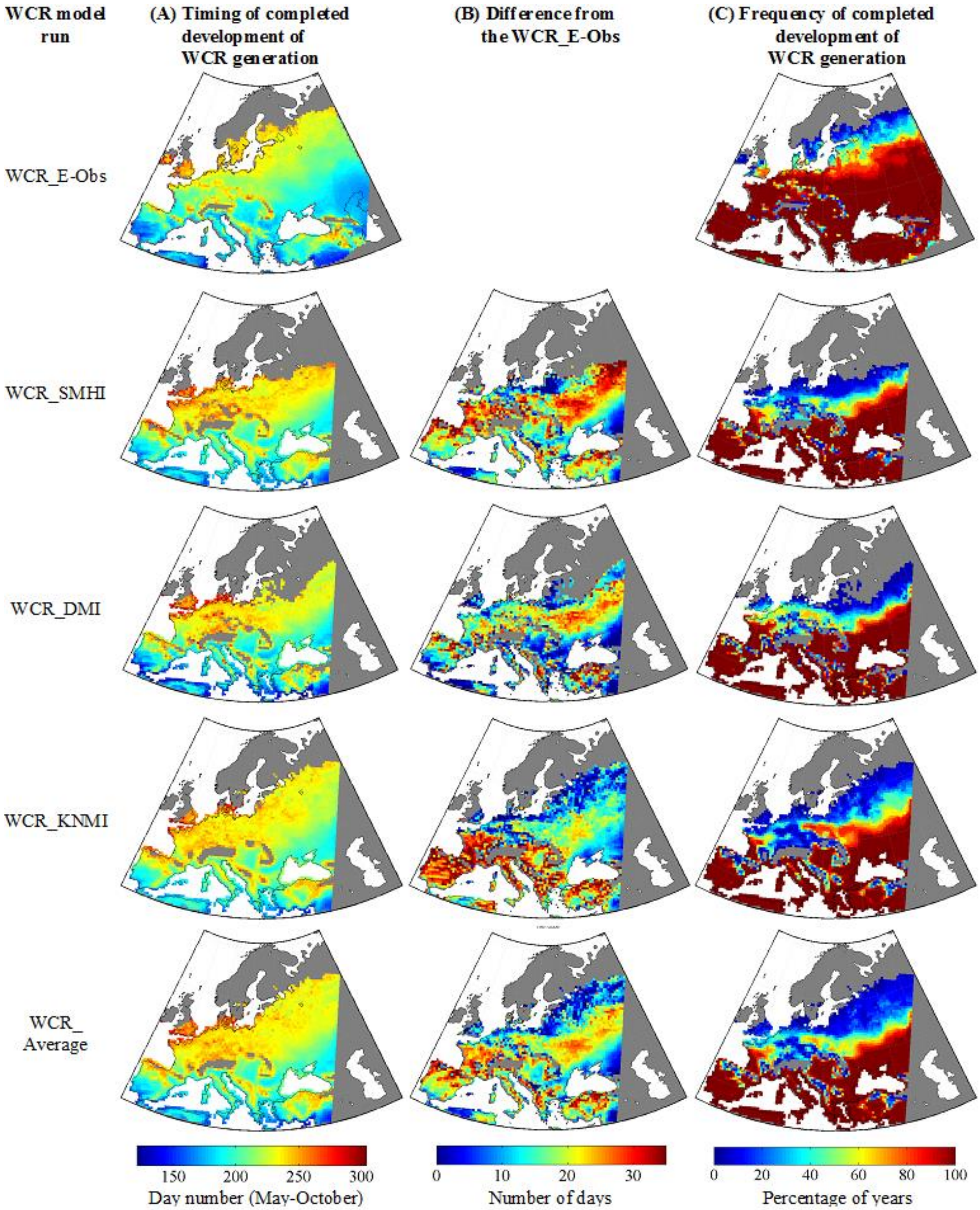

Figure 3 *(A) Average day of the year when the temperature requirements for completed development of WCR generation are fulfilled during 1981-2005. (B) Difference between the modelled timing and timing produced by the WCR_E-Obs during 1981-2005. (C) Percentage of years when the temperature requirements are fulfilled during 1981-2005.*

4.1.2 Regional details of the WCR model performance

The regionally averaged biases in mean timing of completed development of WCR generation for multiple impact model simulations with regard to the WCR_E-Obs during the period of 1981-2005 are illustrated in Figure 4. In all regions, the average date for the fulfillment of temperature requirements generated by individual ensemble members and ensemble average is later than that of the WCR_E-Obs. However, the impact model performance varies depending on both region and simulation.

It is worth noting that numerical analysis regarding the output from WCR model simulations, driven by climate model data, in northern regions, such as BI, SC and NE, during the reference period hereinafter is based on data from a small portion of corresponding region due to significant underestimation of the northward extension of area suitable for the WCR development.

In general, a lower bias of 5-10 days for most impact model runs is found in BI and NE, whereas a greater bias of 19-24 days is typical for FR (Fig. 4). Going through the list of individual simulations the following is observed: the WCR_SMHI gives a relatively large overestimation in all regions, with a bias of 10-16 days in the north (BI, SC, NE) and south (MD, IP), and a bias of 18-24 days in the rest of the regions (ME, EE, FR). The WCR_DMI shows a slight overestimation of 2-4 days in MD and NE, a more pronounced overestimation of 8 days in BI and IP and of 16-19 days in the mid-latitudes (EE, ME, FR), and the largest overestimation of 32 days in SC. The WCR_KNMI exhibits a small deviation from the WCR_E-Obs of 5-6 days in the northern regions (BI, NE except for SC), a larger difference of 13-16 days in MD, IP, ME and EE, and the largest deviation of 26 days in FR. The WCR_Average substantially levels out the regional biases of the individual ensemble members resulting in a reduced difference from the WCR_E-Obs. However, the ensemble average preserves region specific biases, varying between one to three weeks.

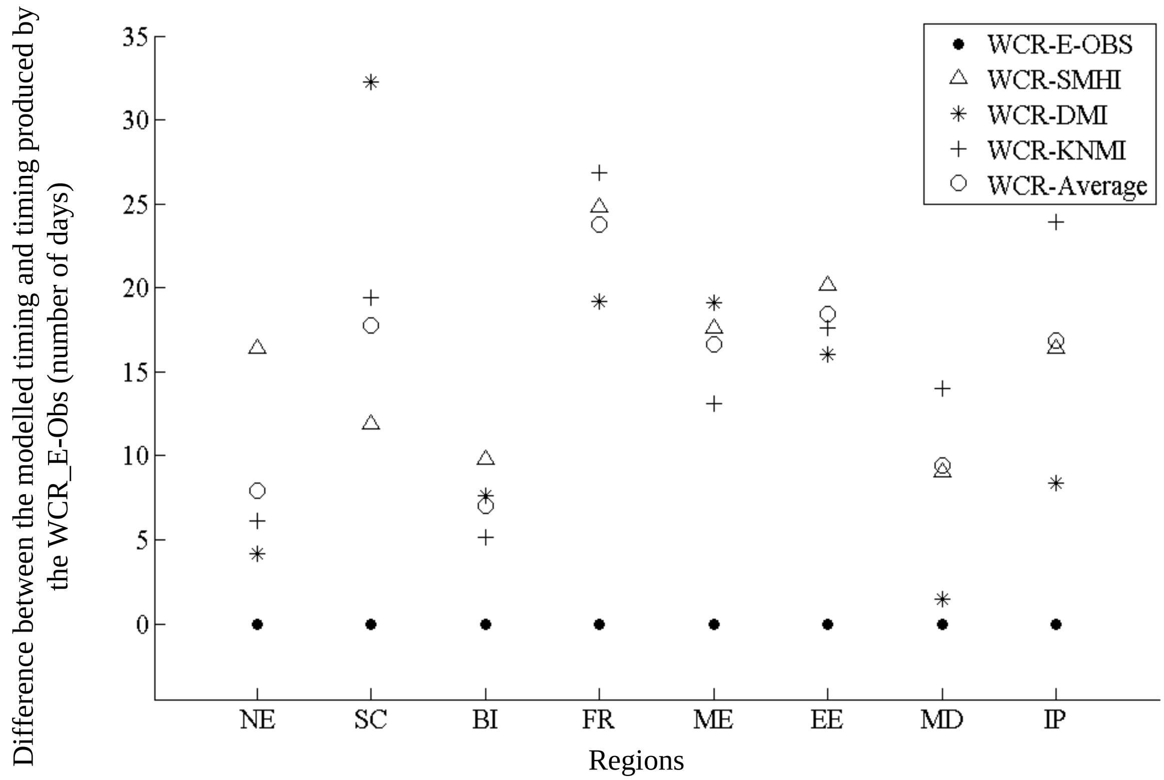

Figure 4 *Regional mean bias in modelled timing of completed development of WCR generation for each ensemble member and the WCR_Average with respect to the WCR_E-Obs during the period of 1981-2005.*

The distributional characteristics of the WCR model results obtained from the different simulations in each region over the period of 1981-2005 is given in Figure 5. All the WCR model runs show a good ability to capture an interannual variation in timing of the completed development of WCR generation in majority of regions with the exceptions of the northern regions (NE, SC). Nevertheless, the median and the maximum value (late timing) is almost always shifted towards the later date in comparison with the WCR_E-Obs.

According to the WCR_E-Obs, all regions except for the northern regions (NE, SC, BI) can sustain the WCR permanent population (Fig. 5). However, the WCR model runs driven by climate model data give a different outcome. In this regard, the distortion of frequency of years, in which the temperature requirements for the development of WCR generation are fulfilled, indicates the WCR model sensitivity to the variability in climate model data. The impact of climatic variability on the WCR model results is the least pronounced in the southern regions (MD, IP), where the climate is warm enough to support the insect development almost in all years. The sensitivity of the WCR model increases northward as the difference in frequency of years between the individual ensemble members and the WCR_E-Obs becomes more evident. The low percentage of years (i.e. few years contribute to the distribution of timing) also reduces the range in timing between the earliest and latest date, as it can be seen in some impact model simulations in the northern regions (NE, SC).

A noticeable feature in all the WCR model simulations within certain regions (FR, EE, MD, IP) is the presence of a considerable amount of cold outliers (late timing), likely introduced by costal climatic conditions (Fig. 5).

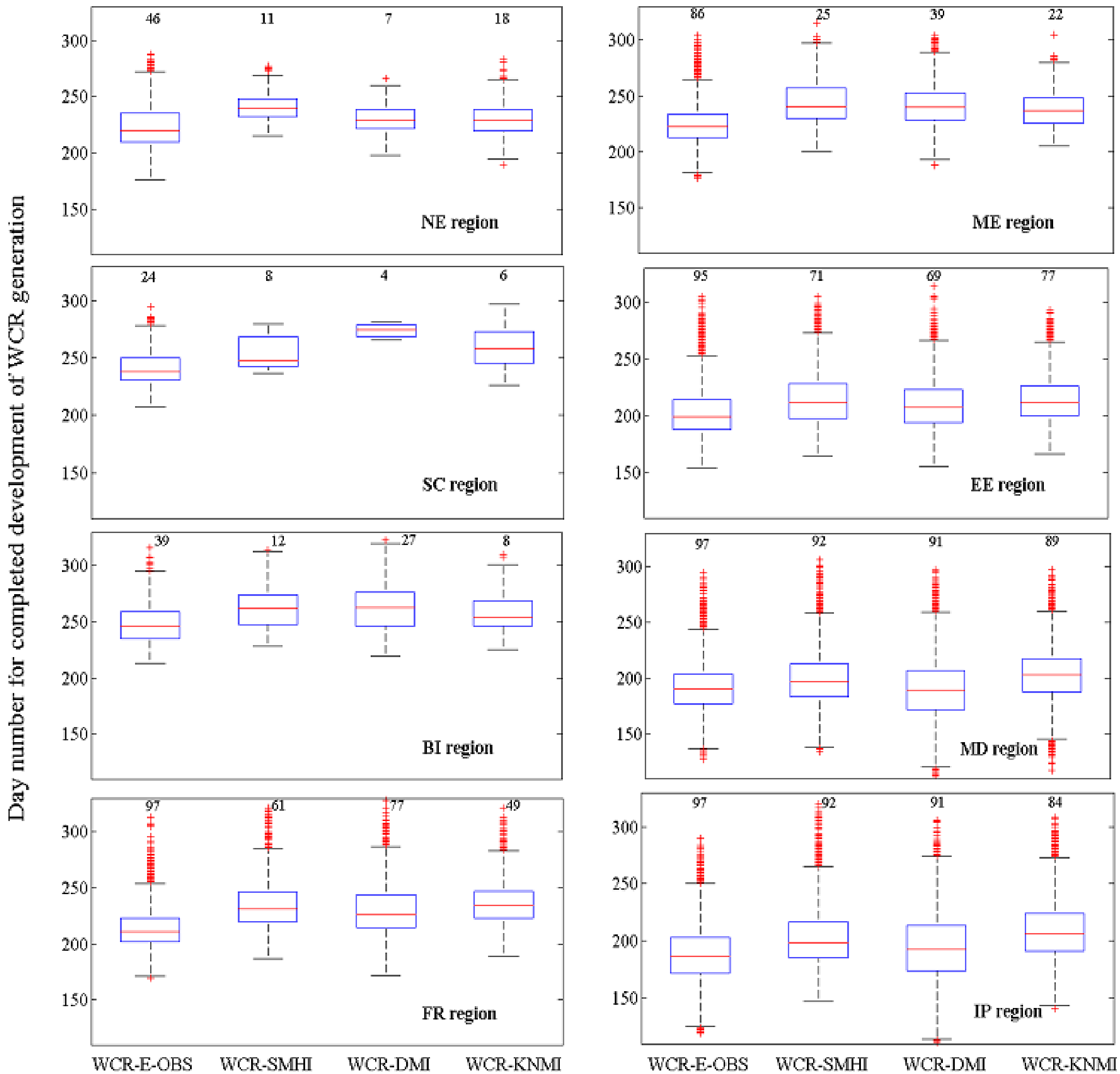

Figure 5 *Descriptive statistics of the WCR model results in every region during the period of 1981-2005. The boxplots show the distribution of timing of completed development of WCR generation. The blue boxes represent the middle 50% of data with the median (red line), upper and lower quartile. The lower and upper whiskers extend to the minimum and maximum values, respectively. The lower and upper outliers (red crosses) indicate values less than 2/3 time of lower quartile and more than 2/3 time of upper quartile, respectively. The number above each box gives the percentage of years when the temperature requirements are fulfilled.*

The regional mean timing and frequency of years of completed development of WCR generation during the period of 1981-2005 are summarized in Table 2. According to all the WCR model simulations, the timing gradually changes towards the later date and the frequency of years decreases, moving from the southern to northern European regions. However, the frequencies produced by the impact model runs with climate model data are usually lower compare to those of the WCR_E-Obs. The effect is pronounced for all regions except for the southern ones.

Table 2 Regional summary statistics for every WCR model run during the period of 1981-2005. The upper number in each table field indicates the regional average day of the year when the temperature requirements for completed development of WCR generation are fulfilled, and the lower number denotes the percentage of years when the temperature requirements are fulfilled.

WCR model	**Region**							
run	**NE**	**SC**	**BI**	**FR**	**ME**	**EE**	**MD**	**IP**
WCR_E-Obs	228	242	254	215	227	201	193	190
	46	24	39	97	86	95	97	97
WCR_SMHI	242	254	264	239	245	221	202	207
	11	8	12	61	25	71	92	92
WCR_DMI	230	274	262	234	246	217	195	199
	7	4	27	77	39	69	91	91
WCR_KNMI	232	261	259	241	240	218	207	214
	18	6	8	49	22	77	89	84
WCR_Average	234	260	261	238	244	219	203	207
	12	6	15	62	27	71	88	88

4.2 WCR model performance during future periods

4.2.1 WCR model future projections for the scenario RCP4.5

The future projections of the WCR model for the scenario RCP4.5 based on the WCR_Average are presented in Figure 6. There is a gradual change in timing of completed development of WCR generation towards an earlier date over Europe under the future temperature (Fig. 6A). The area that fulfills the temperature requirements is projected to extend further north, covering a considerable part of BI, SC and NE. However, a northward extension may be ceased and shrunken in SC and NE in 2071-2100 more likely due to the character of the forcing scenario, according to which CO_2 equivalent concentration and consequently temperature become stable in a given time period.

A climate change signal is determined by the average difference in timing for the periods of 2011-2040, 2041-2070 and 2071-2100 in comparison with 1981-2005 (Fig. 6B). The WCR_Average shows that the development of adult insect may occur an approximately one week earlier in EE, FR, and MD in 2011-2040 than in 1981-2005. The change in timing increases during 2041-2070, reaching about 12 days in MD, two weeks in EE and 17 days in FR and north-west of IP. In 2071-2100, the difference may be up to one week in NE and ME, up to two weeks in MD, and around 17-20 days in EE and FR. Furthermore, the climate change signal cannot be assessed for Sweden and Finland due to the absence of corresponding numerical values in the reference period.

The future projections of frequency of years when the temperature requirements for development of adult WCR are fulfilled (Fig. 6C) reveal a gradual northward shift of the northern border of distributional range of WCR during the 21st century. Therefore, in 2071-2100, the temperature requirements may be fulfilled in 95-100% of years in MD, FR and EE, indicating establishment of the permanent WCR population in these regions. In ME suitable temperature conditions may take place in 80% of years, allowing occurrence of the permanent insect population. With regard to BI and SC, only the most southern parts of these regions may experience high enough frequencies of years around 75-80%, enabling them to sustain a permanent population. For major parts of BI, SC and NE just some years would be suitable for the WCR development.

It should be noted, that the southern and northern European regions display opposite dynamics in respect to timing and frequency of years of completed development of WCR generation (Fig. 6). Thus, the area in the south experiences stronger climate change signal expressed as more pronounced change in timing during the future periods compare to the reference period, while the area in the north undergoes future shifts in frequencies.

The future projections of the individual ensemble members for the RCP4.5 are given in appendix A.

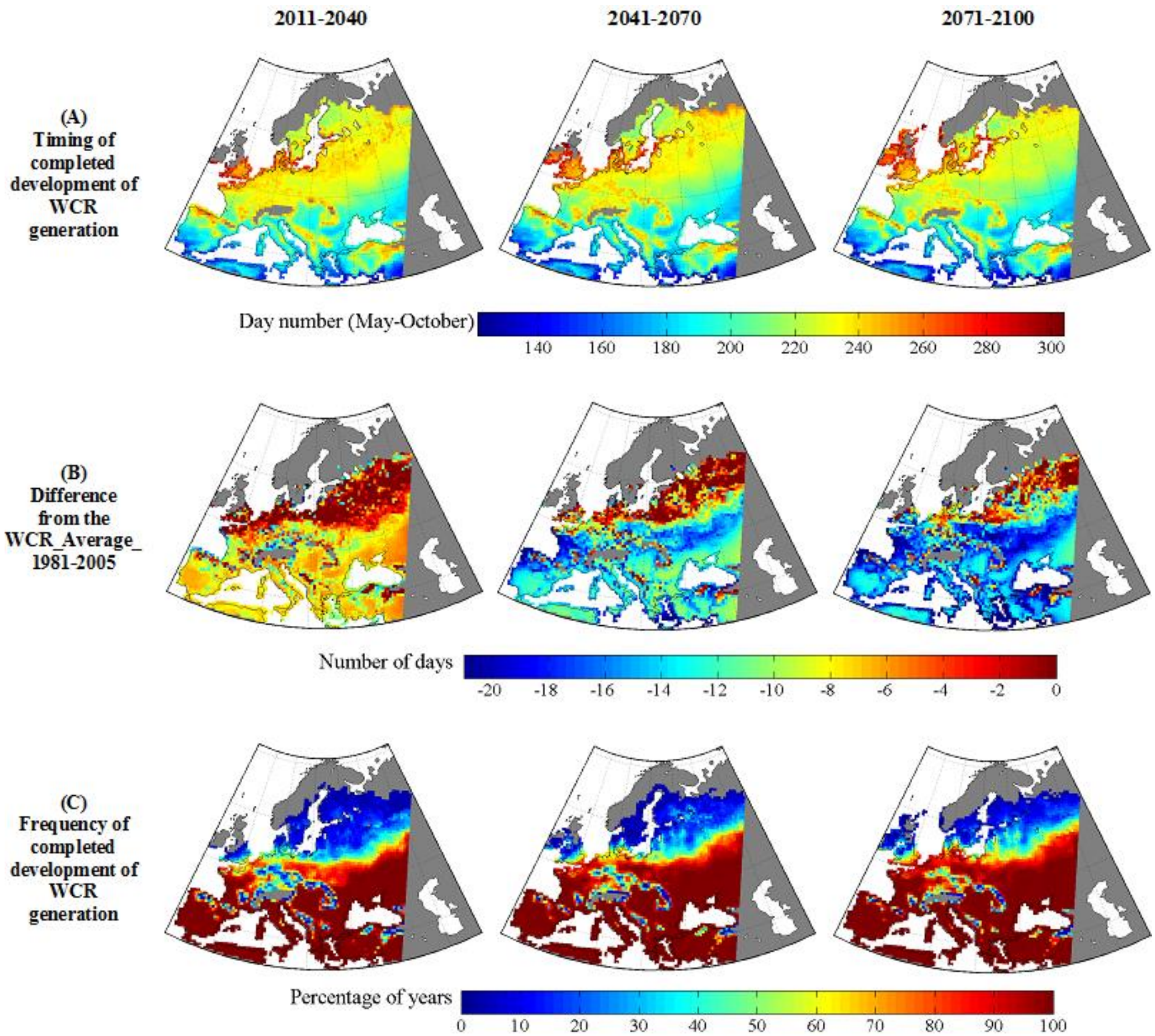

Figure 6 *Results of the WCR_Average for the scenario RCP4.5 during the periods of 2011-2040, 2041-2070 and 2071-2100: (A) Average day of the year when the temperature requirements for completed development of WCR generation are fulfilled. (B) Difference between the modelled future timing and timing modelled by the WCR_Average_1981-2005. (C) Percentage of years when the temperature requirements are fulfilled.*

4.2.2 WCR model future projections for the scenario RCP8.5

The future projections of the WCR model for the scenario RCP8.5 based on the WCR_Average are displayed in Figure 7. The change in timing of completed development of WCR generation towards an earlier date (Fig. 7A) is accelerated over the whole European domain in comparison with the RCP4.5 (Fig. 6A). An area that fulfills the temperature requirements is projected to enlarge towards the northern latitudes, reaching 70^{o}N in 2071-2100.

A climate change signal is assessed by calculating the average difference in timing between the periods of 2011-2040, 2041-2070, 2071-2100 and the reference period (Fig. 7B). The obtained results are similar to that for the RCP4.5 during the period of 2011-2040. That is about one week earlier completion of the development of WCR generation in EE, FR and MD as well as no changes in ME. The change in timing becomes more distinct during 2041-2070. Thus, the temperature requirements may be fulfilled up to one week earlier in ME, up to two weeks earlier in EE and MD, and up to three weeks earlier in FR and northern part of IP. The drastic changes in timing of about one month in EE and MD, and 35-40 days in FR and northern part of Iberian Peninsula are projected for the period of 2071-2100. Besides, the climate change signal cannot be evaluated for Sweden and Finland because of a lack of corresponding numerical values in the reference period.

The future projections of frequencies of years of completed development of WCR generation (Fig. 7C) show a strong shift of the northern limit of occurrence of WCR population, reaching 55^{o}N by the end of 21st century. Almost every year in the area south of 55^{o}N can be suitable for the development of WCR generation in 2071-2100. Opposite patterns of dynamics for timing and frequency of years between southern and northern parts of Europe observed in the RCP4.5 hold true for the RCP8.5.

The future projections of the individual ensemble members for the RCP8.5 are given in appendix B.

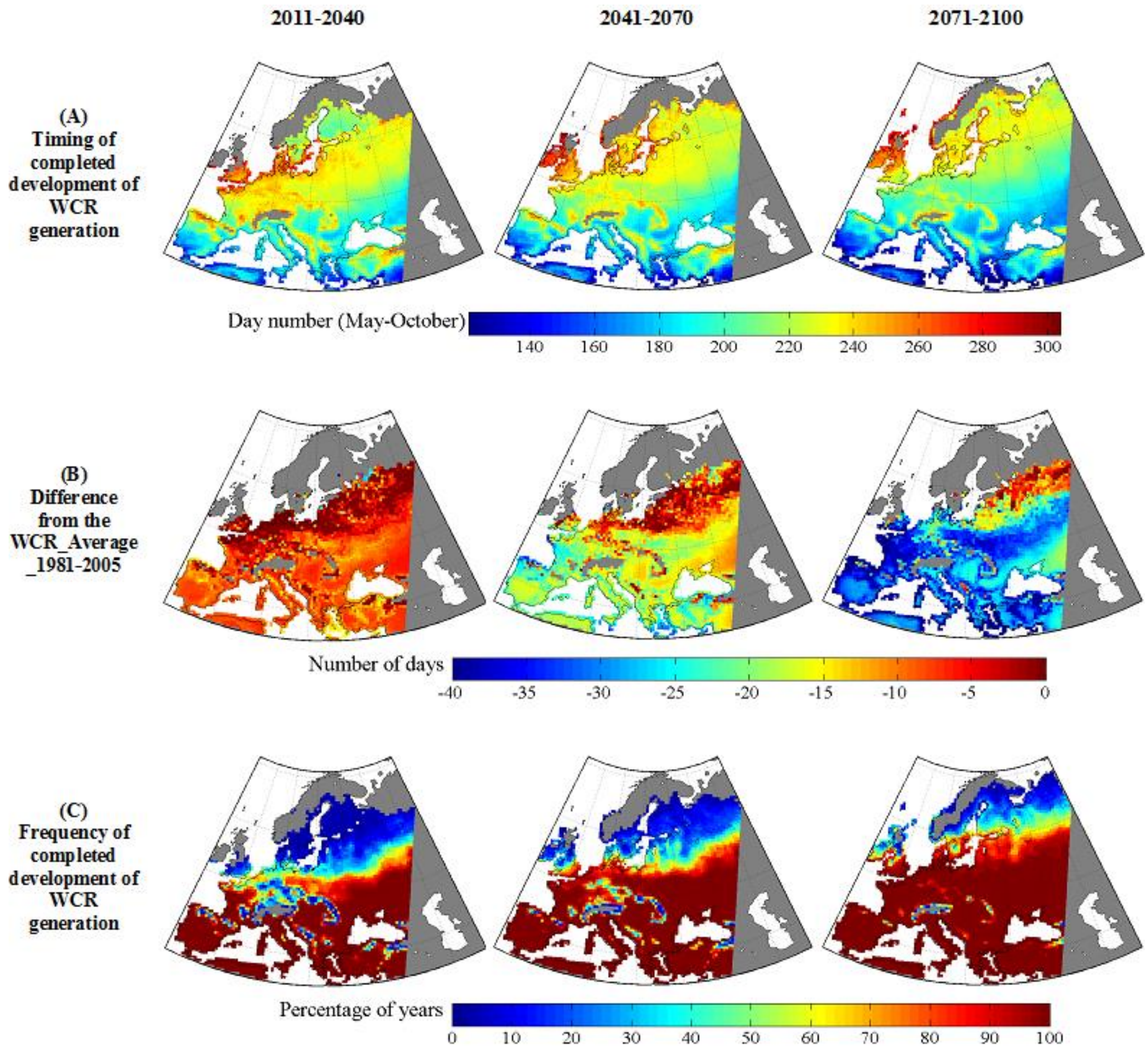

Figure7 *Results of the WCR_Average for the scenario RCP8.5 during the periods of 2011-2040, 2041-2070 and 2071-2100: (A) Average day of the year when the temperature requirements for completed development of WCR generation are fulfilled. (B) Difference between the modelled future timing and timing modelled by the WCR_Average_1981-2005. (C) Percentage of years when the temperature requirements are fulfilled.*

5 Discussion

The current study makes use of an ensemble of climate model data in order to assess the effect of increased temperatures on the WCR activity and distribution in Europe during the 21st century. The impact model simulations show that the temperature requirements for the development of adult WCR may be fulfilled earlier and over a larger area in 2011-2100 in comparison with 1981-2005. The frequency of years in which the temperature requirements are fulfilled is projected to increase, allowing the WCR to spread into the northern European regions and establish a permanent population.

5.1 WCR model performance during reference period

Evaluation of the WCR model using the E-Obs data set as observational reference for the period of 1981-2005 (Fig. 3 and 4) shows that each ensemble member tends to overestimate the average day of the year and underestimate the percentage of years, when the temperature requirements for completed development of WCR generation are fulfilled, over a considerable part of Europe. In general, an overestimation of regional modelled timing by individual ensemble member ranges from 2 to 32 days (Fig. 4 and Table 2), while the northward extension of frequency of years is underestimated in the range of 5-10^{o} of latitude (Fig. 3). However, the magnitude of difference depends on region as well as driving climate model data set, considering latter as the main source of bias. Hence, the information about biases in RCMs involved in this study was derived from Kotlarski et al. (2014), which provides evaluation of each RCM within different European regions applying the lateral boundary conditions from a high quality global meteorological reanalysis product ERA-Interim.

According to Kotlarski et al. (2014), there is a negative bias (up to –2^{o}C) for the majority of RCMs in most seasons and regions, which is reflected by the overall impact model performance (Fig. 3). Regarding the regional details and mean summer temperature, all three RCMs have a weak cold bias of about 1^{o}C in BI, FR (except for SMHI model which has a warm bias of 0.6^{o}C), ME and EE, and a stronger cold bias of around 2^{o}C in SC (except for KNMI model which has a bias of –1^{o}C). These regional model biases are consistent with the bias pattern of the corresponding impact model runs (Fig. 4), indicating the translation of biases inherent in RCM to the impact model. Moreover, all RCMs display either a slight warm bias of approximately 1^{o}C or absence of bias in IP and MD, however these patterns are not followed by the corresponding impact model simulations (Fig. 4). This phenomenon can be explained by the influence of GCM providing boundary conditions to RCMs. That is, changes in large-scale circulation over the coastal regions, IP, MD and FR in particular, may to a great extent induce regional changes (Déqué et al. 2007, Déqué et al. 2012) with a further propagation into the impact model.

In order to reduce biases in individual impact model simulations, introduced by climate model data, ensemble average has been addressed. Since the WCR model is driven by climate model data on a daily time step, averaging was done as later as possible in the process, i.e. mean of (WCR_SMHI + WCR_DMI + WCR_KNMI) was taken, according to the recommendations of RCM developer from SMHI (based on personal communication). Ensemble average produces more accurate results than individual ensemble members due to cancelling out extreme biases from individual runs. Therefore, the WCR_Average overestimates the regional timing and underestimates the northward extension of frequency of years of completed development of WCR generation within more narrow ranges, 6-23 days (Fig. 4 and Table 2) and 5-7^{o} of latitude (Fig. 3), respectively. However, such biases are still large enough, and so should be taken into account while interpreting the future projections of the impact model.

Complementary information about the influence of climate data on the impact model performance can be extracted from the boxplots (Fig. 5). All ensemble members show a relatively good agreement with each other in representing interannual variation in timing of the completed development of WCR generation in most of the regions, as all corresponding RCM have been run under boundary conditions from the same GCM. In addition, regional difference in percentage of years, suitable for the fulfillment of temperature requirements, between individual ensemble members and the WCR_E-Obs can serve as an indication of the impact model sensitivity to the variation in climate model data.

5.2 WCR model future projections

An analysis of future projections of the WCR model based on the ensemble average for the periods of 2011-2040, 2041-2070 and 2071-2100 (Fig. 6 and 7) shows that increased temperature may have a significant impact on the WCR development and distributional range in Europe by the end of the 21st century. This study simplifies the WCR life cycle (Fig. 1) by considering the fulfillment of temperature requirements for the complete development of adult individual, since the insect dispersal (movement to the new territories) happens due to adult flight. Usually, to form a new population more than one gravid adult female is needed (Meinke et al. 2009).

According to both scenarios, RCP4.5 and RCP8.5, the abovementioned temperature requirements may be satisfied in the earlier dates and over the extended territory in future compare to the reference period, along with a stronger climate change signal for the RCP8.5 (Fig. 6 and 7). However, the possibility of WCR to establish a permanent population depends on the percentage of years in which the temperature requirements are fulfilled. Present study considers 75% of years as a lower bound for the WCR population establishment due to the ability of eggs to withstand more than one winter in a diapause stage (Gray et al. 2009). In this regard, although the shift in timing is projected to be more pronounced in the southwestern parts of Europe, this area is already warm enough to support the WCR development during all years. On the other hand, the central, eastern and northern European regions may experience an increase in percentage of years suitable for the development of WCR generation, resulting in the northward expansion of the WCR distributional range. Thus, by the end of the 21st century for the scenarios RCP4.5 and RCP8.5, the northern limit of the WCR distribution is projected to reach approximately 53^{o}N and 55^{o}N, respectively. Taking into account the underestimation in the northward extension of frequency of years during the reference period (Fig. 3C), the northern limit of the WCR distribution should be shifted further north than 53^{o}N or 55^{o}N in future periods. Therefore, the risk of WCR settlement in the northern parts of Europe, including British Isles, Scandinavia and Baltic countries, is high during the second half of the 21st century, most notably in 2071-2100. This information should be communicated to the parties concerned in order to adapt the WCR management practices to the changing climatic conditions.

5.3 Uncertainties associated with observational data

Since the impact model output is comprised by the values averaged over a grid cell, it is more appropriate to evaluate the performance of impact model against gridded observed data (obtained through interpolation of irregularly spaced meteorological stations data to a regular grid), rather than point values (Haylock et al. 2008, Kyselý and Plavcová 2010). The European daily high-resolution gridded data set, the E-Obs, was used as an observational reference in the present study. Although, the E-Obs is developed on basis of the largest European network of stations and the interpolation method applied, namely global kriging, was selected after thorough evaluation of other methods, the data set exhibits a number of potential limitations and uncertainties (Hofstra et al. 2009).

An important limitation occurs from the underlying station network, whose spatial density is insufficient for a high resolution gridding over a considerable part of Europe. Thus, an interpolation procedure leads to smoothing of the spatial variability of climatic parameters. However, this is more pronounced for precipitation than temperature. Overall, an interpolation accuracy decreases with the decrease in station network density and in areas of complex topography (Haylock et al. 2008, Hofstra et al. 2009).

In addition, other sources of observational uncertainty may include uncertainty related to measurements (errors from thermometer reading), incorrect information on station location, inhomogeneity in the station time series, or urbanization effect (from urban stations, located near city centers and thereby influenced by urban heat Isles) (Hofstra et al. 2009, Kyselý and Plavcová 2010). However, it is assumed that uncertainties associated with observational data are relatively small compare to other kinds of uncertainties arisen during the process of impact modeling. Therefore, an observational uncertainty is often disregarded in evaluation of the impact model performance (Gleckler et al. 2008), as in case of the current study.

5.4 Uncertainties associated with climate model data

Regarding the uncertainties related to regional and global climate simulations, a number of studies have been carried out, applying different combination of RCM-GCM within an ensemble (Christensen and Christensen 2007, Déqué et al. 2007, Kendon et al. 2010, Déqué et al. 2012) approach. According to their main findings, the contribution of different RCMs to the spread in projected temperature is more relevant in continental parts of Europe and also during the first half of the 21st century. Additionally, sampling boundary conditions from several GCMs is more important for the variation in projected temperature in coastal European regions as well as during the second half of the 21st century. The suggestion for the impact assessment studies using climate model data was to employ the output from such a large set of RCMs, which would be comparable to the number of driving GCMs, but not less than two both for RCMs and GCMs

In the present study the ensemble of climate model data represents output from three different RCMs forced by the same GCM. The possibility to use more comprehensive set of RCM-GCM was restricted by the data availability and time required for data processing by the impact model. Although the current ensemble does not cover the global model uncertainty, it allows to explore the influence of different RCMs on the impact model performance.

In addition, this study enables to capture the forcing scenario uncertainty by running the impact model with climate model data representing two different RCP scenarios, RCP4.5 and RCP8.5, and computing the ensemble average for each of them. Analysis of the future projections of WCR_Average reveals that the choice of forcing scenario is less important during the period of 2011-2040, since the WCR_Average outputs for the RCP4.5 and the RCP8.5 are similar in a given time period. However, the forcing scenarios become significant source of uncertainty during the later periods, as the differences in the WCR_Average projections between the RCP4.5 and RCP8.5 get more pronounced towards the end of the 21st century. It is noteworthy that additional impact model runs for two other RCPs, i.e. RCP2.6 and RCP6.0, would give a broader range of projected output, i.e. greater uncertainty, at least for the second half of the 21st century (Déqué et al. 2007, IPCC 2013).

5.5 Uncertainties associated with the WCR model

There is uncertainty regarding the impact model parameters, i.e. the WCR model outcome depends on the choice of lower developmental threshold and SET. In present study, the impact model has been parameterized according to the results of a field experiment for the WCR population in Central Europe. Although the uncertainty remains in relation to the accuracy of experimentally determined temperature requirements (12.5^{o}C and 415 DD), these values are assumed to be representative for other European populations. The assumption is based on the analysis of genetic variability within and between different European outbreaks (Miller et al. 2005, Ciosi et al. 2008), which indicates that majority of them originates from the common source population. However the local differences in temperature requirements may exist between unstudied populations. Moreover, the adaptations to local thermal conditions at higher latitudes, such as decreased lower developmental threshold and increased SET (Honek 1996), may appear in newly formed WCR population in northern regions.

5.6 Implications of the WCR model projections

Despite the uncertainties in the future WCR model projections are high, especially regarding the northern limit of the WCR distributional range, it is more likely that future temperature conditions will be suitable for the WCR establishment in the northern parts of Europe, including British Isles, Scandinavia and Baltic countries. Taking into account a long-distance movement of adult WCR (can fly up to 24 km) (Carrasco et al. 2010), a great reproductive potential of adult female and an exceptional ability to adapt to new environmental conditions, the risk of the WCR spread into new areas is high. However, a successful invasion will depend on the number of factors, such as a persistent invasion front (occurring every year) from the neighboring territories, availability of host plant and absence of topographical barriers. Since the WCR needs continuous maize productions to complete its life cycle, an increase of crop rotation fields in areas ahead of the invasion front may have preventive effect on the WCR spread (Meinke et al. 2009). In addition, climate change may affect maize phenology resulting in an alteration of synchrony between the WCR and maize life cycles (Porter et al. 1991), consequently determining the insect future distribution. Although the topographical features may serve as a barriers for the WCR dispersal, they can be overcome, for instance, through roads and railways in mountain valleys or with strong winds blowing over large water bodies (Meinke et al. 2009).

It is important to continuously monitor regions with established WCR populations as well as uninfested territories in order to detect new outbreaks of the WCR and employ containment actions (Kiss et al. 2005). Primarily management measures should include allocation of a buffer zone around each infested field, maize rotation and insecticide treatment within each zone (Carrasco et al. 2010, Sivčev et al. 2012). Thus, since the first detection of the WCR in Serbia, a broad European monitoring network has been developed, supported by the international organizations, such as the International Working Group on *Ostrinia* and Other Maize Pests of the International Organization for Biological Control, the United Nations Food and Agriculture Organization, EPPO, etc. (Kiss et al. 2005).

Considering the possibility of the WCR invasion to Sweden, both consistent insect inflow from northern Germany and Poland and favorable prevailing winds to surmount the Baltic Sea will be necessary. In addition, satisfactory implementation of current eradication measures in Germany and Poland may inhibit the WCR migration to southern Sweden. However, a human-induced dispersal (e.g. transportation via train or airplane) may also occur.

5.7 Recommendations for further research

As it has been discussed earlier, the impact model outputs produced by using climate model data, including the output from ensemble average, deviates to a great extent from those produced by using observation data. This introduces uncertainties to the future impact model projections, highlighting the need to improve the quality of climate model data. However, better performance of the impact model may be achieved by applying more comprehensive ensemble of climate model data as well as data with a higher spatial resolution. The aspects related to the uncertainty in model parameterization should also be taken into account by future research.

This modeling study can be extended by considering effect of other factors on the WCR development, e.g. temperatures exciding upper developmental threshold, influence of cold temperatures on egg survival and impact of dry days on post-diapause eggs. Additionally, the WCR model can be coupled with maize phenology, therefore capturing complex interaction between the WCR, maize and climatic parameters.

6 Conclusions

This study shows that higher temperatures associated with climate change may alter both timing of the WCR development and range of the WCR distribution in Europe during 2011-2100 in comparison with 1981-2005. The temperature requirements for the completed development of WCR generation may be satisfied earlier in the year and over enhanced territory. The frequency of years in which the temperature requirements are fulfilled is projected to increase in central, eastern and northern parts of Europe, indicating a northward extension of the area suitable for the establishment of a permanent WCR population. Interested parties should be informed about possible risks of the WCR spread in order to adjust management practices.

References

Bale, J. S., G. J. Masters, I. D. Hodkinson, C. Awmack, T. M. Bezemer, V. K. Brown, J. Butterfield, A. Buse, J. C. Coulson, and J. Farrar. 2002. Herbivory in global climate change research: direct effects of rising temperature on insect herbivores. Global Change Biology 8:1-16.

Bøssing Christensen, O., M. Drews, J. Hesselbjerg Christensen, K. Dethloff, K. Ketelsen, I. Hebestadt, and A. Rinke. 2007. The HIRHAM Regional Climate Model. Version 5 (beta). Danish Climate Centre, Danish Meteorological Institute.

Carrasco, L., T. Harwood, S. Toepfer, A. MacLeod, N. Levay, J. Kiss, R. Baker, J. Mumford, and J. Knight. 2010. Dispersal kernels of the invasive alien western corn rootworm and the effectiveness of buffer zones in eradication programmes in Europe. Annals of Applied Biology 156:63-77.

Chiang, H. 1973. Bionomics of the northern and western corn rootworms. Annual review of entomology 18:47-72.

Christensen, J. H., and O. B. Christensen. 2007. A summary of the PRUDENCE model projections of changes in European climate by the end of this century. Climatic Change 81:7-30.

Ciosi, M., N. Miller, K. Kim, R. Giordano, A. Estoup, and T. Guillemaud. 2008. Invasion of Europe by the western corn rootworm, Diabrotica virgifera virgifera: multiple transatlantic introductions with various reductions of genetic diversity. Molecular Ecology 17:3614-3627.

Déqué, M., D. Rowell, D. Lüthi, F. Giorgi, J. Christensen, B. Rockel, D. Jacob, E. Kjellström, M. De Castro, and B. van den Hurk. 2007. An intercomparison of regional climate simulations for Europe: assessing uncertainties in model projections. Climatic Change 81:53-70.

Déqué, M., S. Somot, E. Sanchez-Gomez, C. Goodess, D. Jacob, G. Lenderink, and O. Christensen. 2012. The spread amongst ENSEMBLES regional scenarios: regional climate models, driving general circulation models and interannual variability. Climate Dynamics 38:951-964.

Fand, B. B., A. L. Kamble, and M. Kumar. 2012. Will climate change pose serious threat to crop pest management: A critical review? International Journal of Scientific and Research Publication 2:2250-3153.

Gleckler, P. J., K. E. Taylor, and C. Doutriaux. 2008. Performance metrics for climate models. Journal of Geophysical Research: Atmospheres (1984–2012) 113.

Gordh, G., and S. McKirdy, 2013: The Handbook of Plant Biosecurity: Principles and Practices for the Identification, Containment and Control of Organisms that Threaten Agriculture and the Environment Globally. Springerpp.

Gray, M. E., T. W. Sappington, N. J. Miller, J. Moeser, and M. O. Bohn. 2009. Adaptation and invasiveness of western corn rootworm: intensifying research on a worsening pest*. Annual review of entomology 54:303-321.

Haylock, M. R., N. Hofstra, A. M. G. K. Tank, E. J. Klok, P. D. Jones, and M. New. 2008. A European daily high-resolution gridded data set of surface temperature and precipitation for 1950-2006. Journal of Geophysical Research-Atmospheres 113.

Hazeleger, W., C. Severijns, T. Semmler, S. Stefanescu, S. Yang, X. Wang, K. Wyser, E. Dutra, J. M. Baldasano, and R. Bintanja. 2010. EC-earth: a seamless earth-system prediction approach in action. Bulletin of the American Meteorological Society 91:1357-1363.

Hemerik, L., C. Busstra, and P. Mols. 2004. Predicting the temperature-dependent natural population expansion of the western corn rootworm, Diabrotica virgifera. Entomologia experimentalis et applicata 111:59-69.

Hofstra, N., M. Haylock, M. New, and P. D. Jones. 2009. Testing E-OBS European high-resolution gridded data set of daily precipitation and surface temperature. Journal of Geophysical Research: Atmospheres (1984–2012) 114.

Honek, A. 1996. Geographical variation in thermal requirements for insect development. European Journal of Entomology 93:303-312.

Hostetler, S., J. Alder, and A. Allan. 2011. Dynamically downscaled climate simulations over North America: Methods, evaluation, and supporting documentation for users.

IPCC, 2013: Climate Change 2013: The Physical Science Basis. Contribution of Working Group I to the Fifth Assessment Report of the Intergovernmental Panel on Climate Change. [T. F. Stocker, D. Qin, G.-K. Plattner, M. Tignor, S. K. Allen, J. Boschung, A. Nauels, Y. Xia, V. Bex, and P. M. Midgley (eds.)]. Cambridge University Press, Cambridge, United Kingdom and New York, NY, USA,1535 pp, doi: 10.1017/CBO9781107415324.

Jackson, J. J., and N. C. Elliot. 1988. Temperature-dependent development of immature stages of the western corn rootworm, Diabrotica virgifera virgifera (Coleoptera: Chrysomelidae). Environmental Entomology 17:166-171.

Jacob, D., J. Petersen, B. Eggert, A. Alias, O. B. Christensen, L. M. Bouwer, A. Braun, A. Colette, M. Déqué, and G. Georgievski. 2014. EURO-CORDEX: new high-resolution climate change projections for European impact research. Regional Environmental Change 14:563-578.

Kendon, E. J., R. G. Jones, E. Kjellström, and J. M. Murphy. 2010. Using and designing GCM-RCM ensemble regional climate projections. Journal of Climate 23:6485-6503.

Kiss, J., C. Edwards, H. Berger, P. Cate, M. Cean, S. Cheek, J. Derron, L. Furlan, I. Ivanova, and W. Lammers. 2005. Monitoring of western corn rootworm (Diabrotica virgifera virgifera LeConte) in Europe 1992-2003. Western corn rootworm: ecology and management:29-39.

Kyselý, J., and E. Plavcová. 2010. A critical remark on the applicability of E-OBS European gridded temperature data set for validating control climate simulations. Journal of Geophysical Research: Atmospheres (1984–2012) 115.

Kotlarski, S., K. Keuler, O. B. Christensen, A. Colette, M. Déqué, A. Gobiet, K. Goergen, D. Jacob, D. Lüthi, and E. van Meijgaard. 2014. Regional climate modeling on European scales: a joint standard evaluation of the EURO-CORDEX RCM ensemble. Geoscientific Model Development Discussions 7:217-293.

Lammers, W. 2006. Report of a Pest Risk Analysis. Netherlands Plant Protection Service.

Meijgaard, E. v., L. v. Ulft, G. Lenderink, S. d. Roode, L. Wipfler, R. Boers, and R. Timmermans, 2008: Refinement and application of a regional atmospheric model for climate scenario calculations of Western Europe. [Sl]: Royal Netherlands Meteorological Institute (KNMI)pp.

Meinke, L. J., T. W. Sappington, D. W. Onstad, T. Guillemaud, N. J. Miller, J. Komáromi, N. Levay, L. Furlan, J. Kiss, and F. Toth. 2009. Western corn rootworm (Diabrotica virgifera virgifera LeConte) population dynamics. Agricultural and Forest Entomology 11:29-46.

Miller, N., A. Estoup, S. Toepfer, D. Bourguet, L. Lapchin, S. Derridj, K. S. Kim, P. Reynaud, L. Furlan, and T. Guillemaud. 2005. Multiple transatlantic introductions of the western corn rootworm. Science 310:992-992.

Moss, R. H., J. A. Edmonds, K. A. Hibbard, M. R. Manning, S. K. Rose, D. P. van Vuuren, T. R. Carter, S. Emori, M. Kainuma, T. Kram, G. A. Meehl, J. F. B. Mitchell, N. Nakicenovic, K. Riahi, S. J. Smith, R. J. Stouffer, A. M. Thomson, J. P. Weyant, and T. J. Wilbanks. 2010. The next generation of scenarios for climate change research and assessment. Nature 463:747-756.

Newton, A. C., S. N. Johnson, and P. J. Gregory. 2011. Implications of climate change for diseases, crop yields and food security. Euphytica 179:3-18.

Porter, J., M. Parry, and T. Carter. 1991. The potential effects of climatic change on agricultural insect pests. Agricultural and Forest Meteorology 57:221-240.

Rummukainen, M. 2010. State-of-the-art with Regional Climate Models. Wiley Interdisciplinary Reviews: Climate Change 1:82-96.

Samuelsson, P., C. G. Jones, U. Willén, A. Ullerstig, S. Gollvik, U. Hansson, C. Jansson, E. Kjellström, G. Nikulin, and K. Wyser. 2011. The Rossby Centre Regional Climate model RCA3: model description and performance. Tellus A 63:4-23.

Scherm, H., R. Sutherst, R. Harrington, and J. Ingram. 2000. Global networking for assessment of impacts of global change on plant pests. Environmental Pollution 108:333-341.

Sivčev, I., P. Kljajić, M. Kostić, L. Sivčev, and S. Stanković. 2012. Management of western corn rootworm (Diabrotica virgifera virgifera). Pesticidi i fitomedicina 27:189-201.

Streda, T., O. Vahala, and H. Stredova. 2013. Prediction of Adult Western Corn Rootworm (Diabrotica virgifera virgifera LeConte) Emergence. Plant Protection Science 49:89-97.

Szalai, M., J. P. Komáromi, R. Bažok, J. I. Barčić, J. Kiss, and S. Toepfer. 2011. Generational growth rate estimates of Diabrotica virgifera virgifera populations (Coleoptera: Chrysomelidae). Journal of Pest Science 84:133-142.

Taylor, K. E., R. J. Stouffer, and G. A. Meehl. 2012. An overview of CMIP5 and the experiment design. Bulletin of the American Meteorological Society 93:485-498.

Trudgill, D., A. HONEK, D. Li, and N. Straalen. 2005. Thermal time–concepts and utility. Annals of Applied Biology 146:1-14.

Wesseler, J., and E. H. Fall. 2010. Potential damage costs of Diabrotica virgifera virgifera infestation in Europe–the 'no control'scenario. Journal of Applied Entomology 134:385-394.

Wilde, G. E. 1971. Temperature effect on development of western corn rootworm eggs. Journal of the Kansas Entomological Society:185-187.

Wilstermann, A., and S. Vidal. 2013. Western corn rootworm egg hatch and larval development under constant and varying temperatures. Journal of Pest Science 86:419-428.

Appendices

Appendix A

Future projections of the individual ensemble members for the scenario RCP4.5

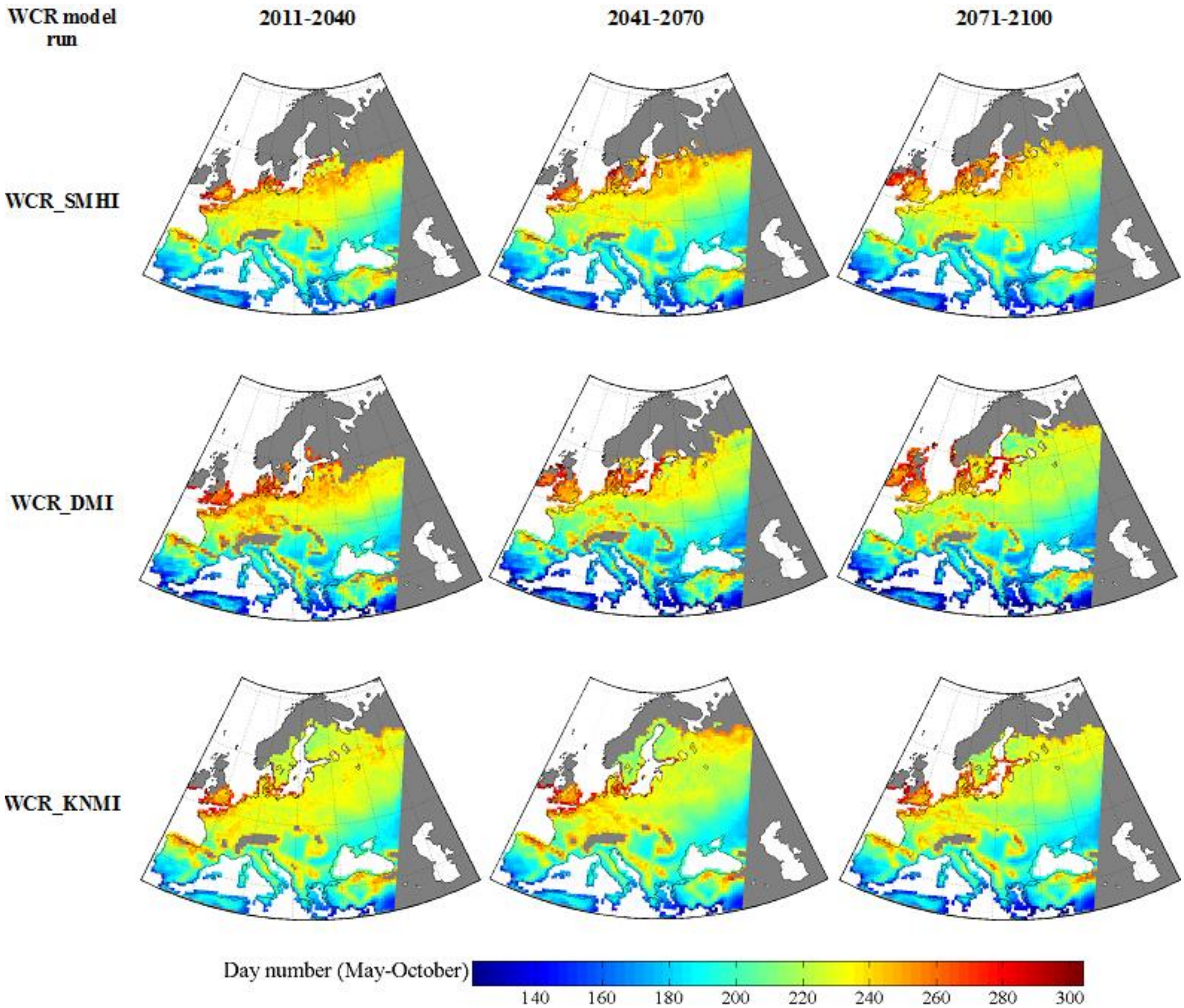

Figure A1 *Average day of the year when the temperature requirements for completed development of WCR generation are fulfilled, produced by the WCR_SMHI, WCR_DMI and WCR_KNMI for the periods 2011-2040, 2041-2070 and 2071-2100.*

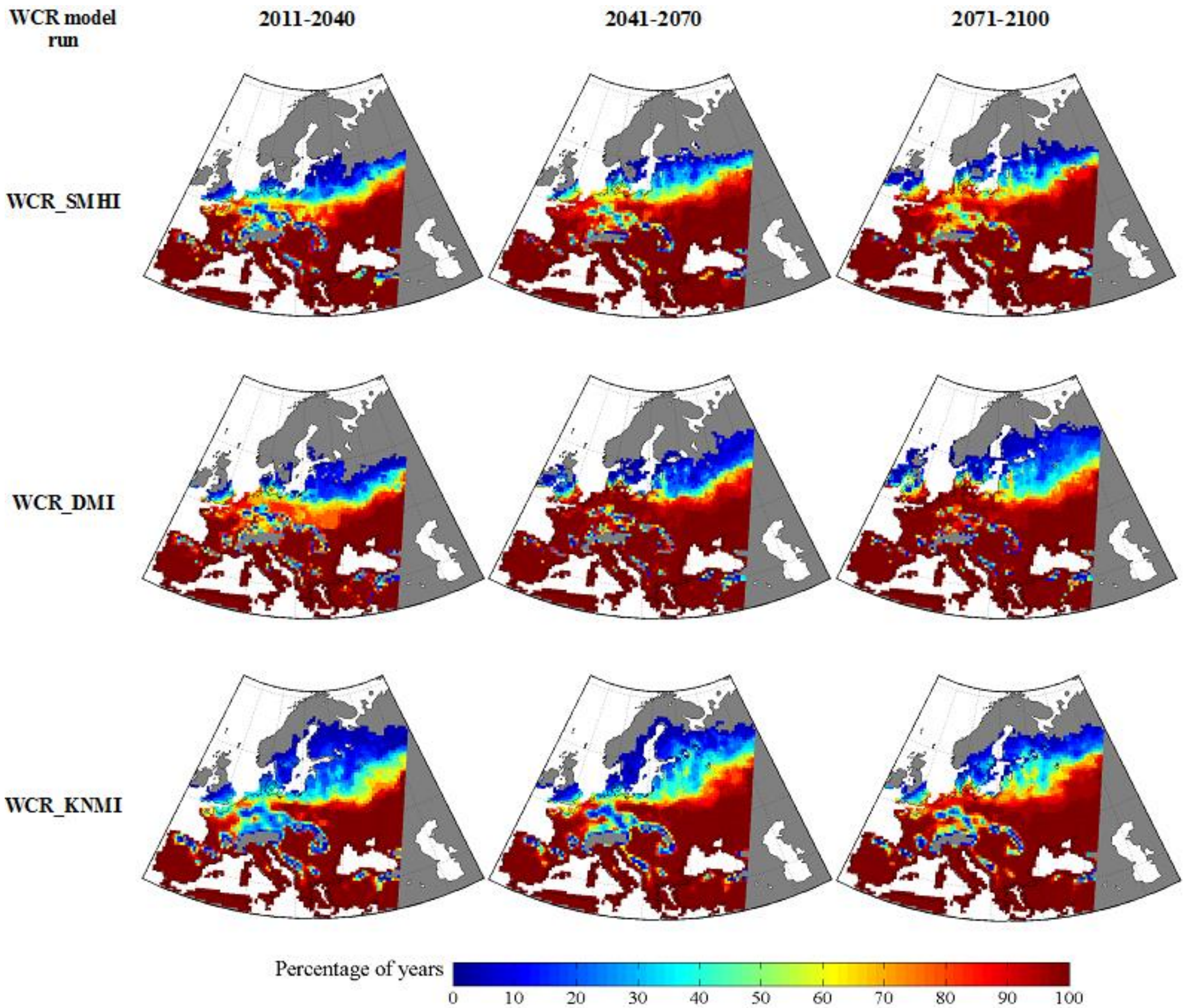

Figure A2 *Percentage of years when the temperature requirements are fulfilled, produced by the WCR_SMHI, WCR_DMI and WCR_KNMI for the periods 2011-2040, 2041-2070 and 2071-2100.*

Appendix B
Future projections of the individual ensemble members for the scenario RCP8.5

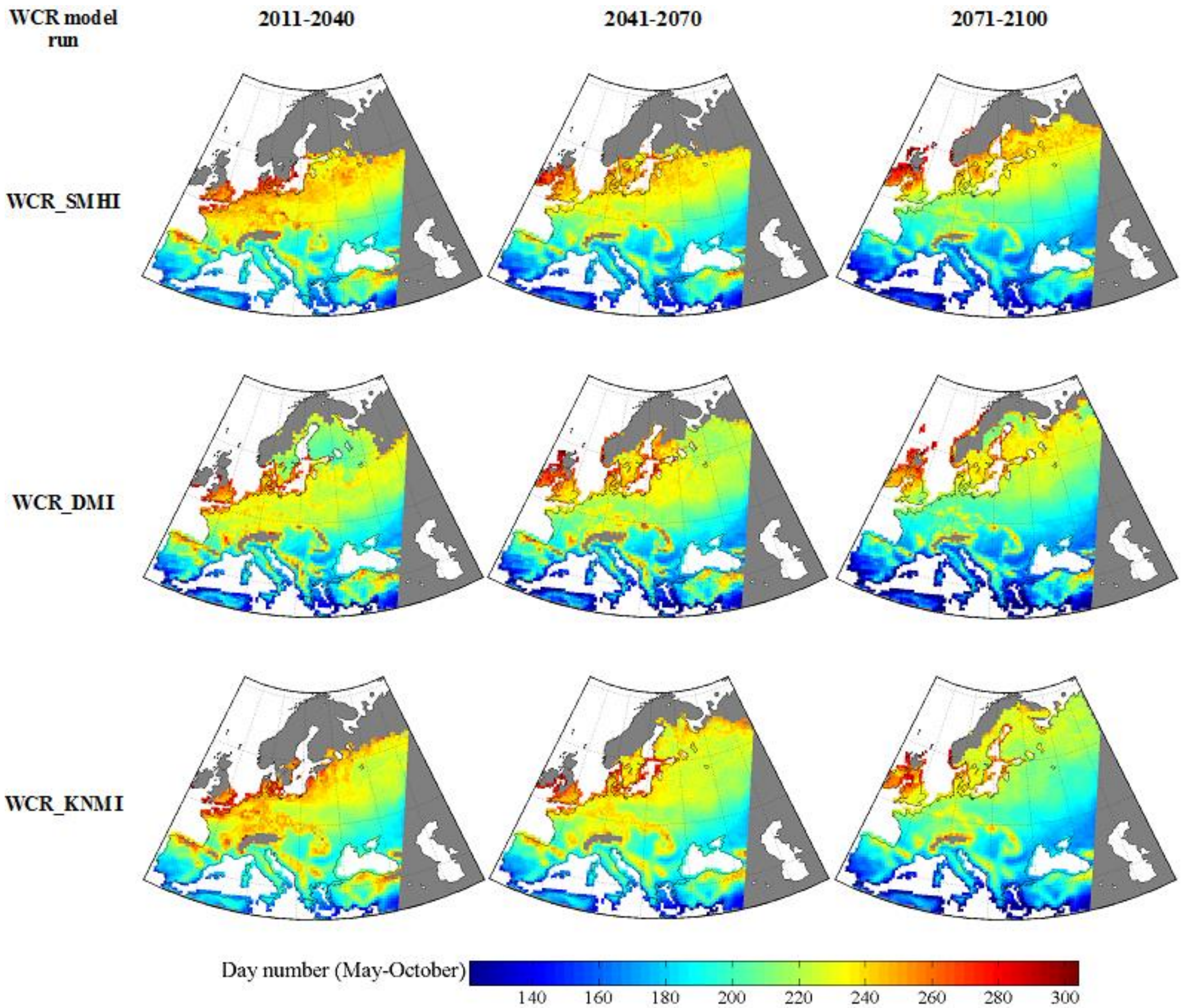

Figure B1 *Average day of the year when the temperature requirements for completed development of WCR generation are fulfilled, produced by the WCR_SMHI, WCR_DMI and WCR_KNMI for the periods 2011-2040, 2041-2070 and 2071-2100.*

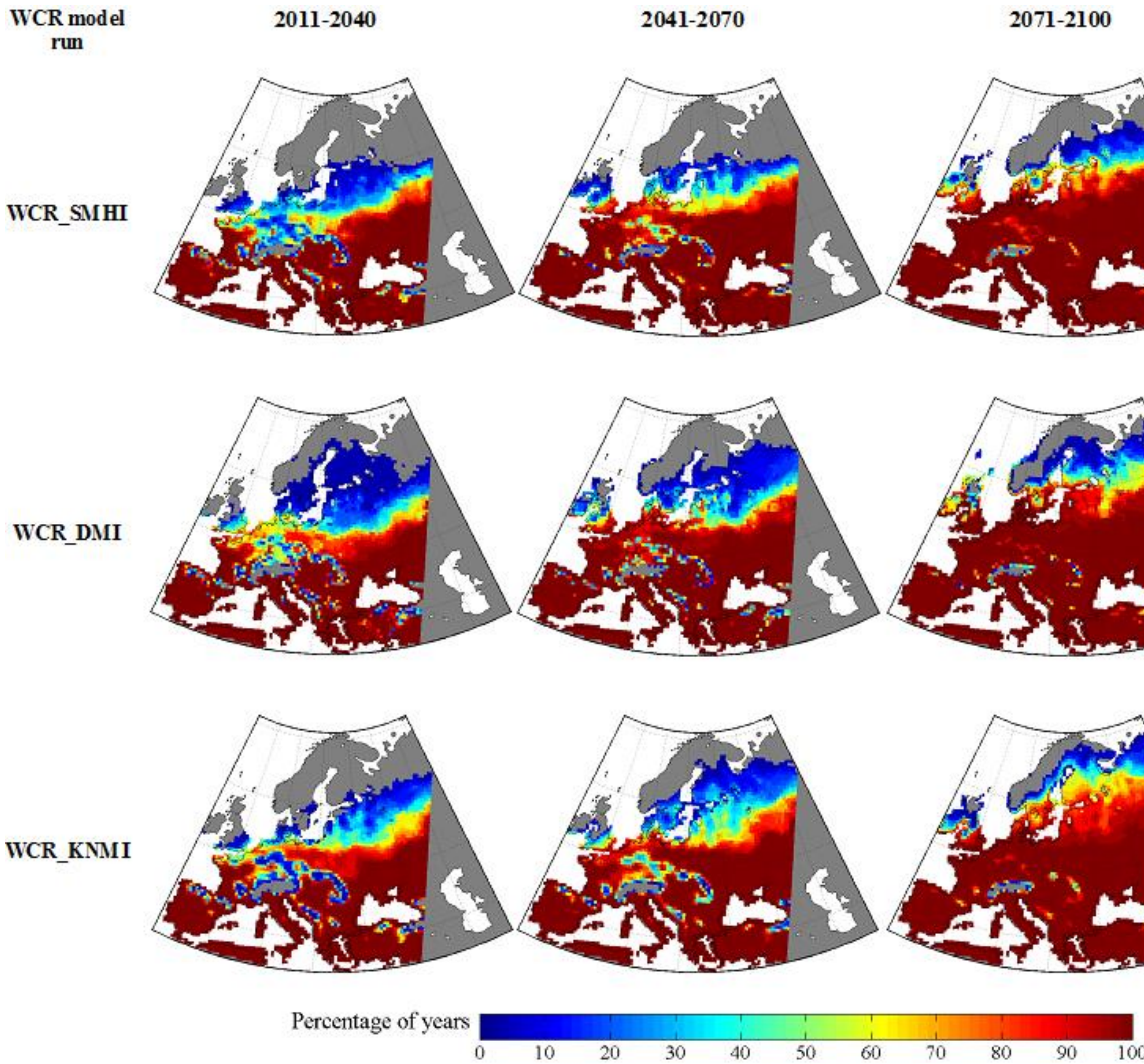

Figure B2 *Percentage of years when the temperature requirements are fulfilled, produced by the WCR_SMHI, WCR_DMI and WCR_KNMI for the periods 2011-2040, 2041-2070 and 2071-2100.*

Institutionen för naturgeografi och ekosystemvetenskap, Lunds Universitet.

Student examensarbete (Seminarieuppsatser). Uppsatserna finns tillgängliga på institutionens geobibliotek, Sölvegatan 12, 223 62 LUND. Serien startade 1985. Hela listan och själva uppsatserna är även tillgängliga på LUP student papers (www.nateko.lu.se/masterthesis) och via Geobiblioteket (www.geobib.lu.se)

The student thesis reports are available at the Geo-Library, Department of Physical Geography and Ecosystem Science, University of Lund, Sölvegatan 12, S-223 62 Lund, Sweden. Report series started 1985. The complete list and electronic versions are also electronic available at the LUP student papers (www.nateko.lu.se/masterthesis) and through the Geo-library (www.geobib.lu.se)

294 Mattias Spångmyr (2014) Development of an Open-Source Mobile Application for Emergency Data Collection
295 Hammad Javid (2013) Snowmelt and Runoff Assessment of Talas River Basin Using Remote Sensing Approach
296 Kirstine Skov (2014) Spatiotemporal variability in methane emission from an Arctic fen over a growing season – dynamics and driving factors
297 Sandra Persson (2014) Estimating leaf area index from satellite data in deciduous forests of southern Sweden
298 Ludvig Forslund (2014) Using digital repeat photography for monitoring the regrowth of a clear-cut area
299 Julia Jacobsson (2014) The Suitability of Using Landsat TM-5 Images for Estimating Chromophoric Dissolved Organic Matter in Subarctic Lakes
300 Johan Westin (2014) Remote sensing of deforestation along the trans-Amazonian highway
301 Sean Demet (2014) Modeling the evolution of wildfire: an analysis of short term wildfire events and their relationship to meteorological variables
302 Madelene Holmblad (2014). How does urban discharge affect a lake in a recreational area in central Sweden? – A comparison of metals in the sediments of three similar lakes
303 Sohidul Islam (2014) The effect of the freshwater-sea transition on short-term dissolved organic carbon bio-reactivity: the case of Baltic Sea river mouths
304 Mozafar Veysipanah (2014) Polynomial trends of vegetation phenology in Sahelian to equatorial Africa using remotely sensed time series from 1983 to 2005
305 Natalia Kelbus (2014) Is there new particle formation in the marine boundary layer of the North Sea?
306 Zhanzhang Cai (2014) Modelling methane emissions from Arctic tundra wetlands: effects of fractional wetland maps
307 Erica Perming (2014) Paddy and banana cultivation in Sri Lanka - A study analysing the farmers' constraints in agriculture with focus on Sooriyawewa D.S. division
308 Nazar Jameel Khalid (2014) Urban Heat Island in Erbil City.
309 Jessica, Ahlgren & Sophie Rudbäck (2014) The development of GIS-usage in

developed and undeveloped countries during 2005-2014: Tendencies, problems and limitations

310 Jenny Ahlstrand (2014) En jämförelse av två riskkarteringar av fosforförlust från jordbruksmark – Utförda med Ekologgruppens enkla verktyg och erosionsmodellen USPED

311 William Walker (2014) Planning Green Infrastructure Using Habitat Modelling. A Case Study of the Common Toad in Lomma Municipality

312 Christiana Marie Walcher (2014) Effects of methane and coastal erosion on subsea-permafrost and emissions

313 Anette Fast (2014) Konsekvenser av stigande havsnivå för ett kustsamhälle- en fallstudie av VA systemet i Beddingestrand

314 Maja Jensen (2014) Stubbrytningens klimatpåverkan. En studie av stubbrytningens kortsiktiga effekter på koldioxidbalansen i boreal barrskog

315 Emelie Norhagen (2014) Växters fenologiska svar på ett förändrat klimat - modellering av knoppsprickning för hägg, björk och asp i Skåne

316 Liisi Nõgu (2014) The effects of site preparation on carbon fluxes at two clear-cuts in southern Sweden

317 Julian Will (2014) Development of an automated matching algorithm to assess the quality of the OpenStreetMap road network - A case study in Göteborg, Sweden

318 Niklas Olén (2011) Water drainage from a Swedish waste treatment facility and the expected effect of climate change

319 Wösel Thoresen (2014) Burn the forest - Let it live. Identifying potential areas for controlled forest fires on Gotland using Geographic Information System

320 Jurgen van Tiggelen (2014) Assimilation of satellite data and in-situ data for the improvement of global radiation maps in the Netherlands.

321 Sam Khallaghi (2014) Posidonia Oceanica habitat mapping in shallow coastal waters along Losinj Island, Croatia using Geoeye-1 multispectral imagery.

322 Patrizia Vollmar (2014) The influence of climate and land cover on wildfire patterns in the conterminous United States

323 Marco Giljum (2014) Object-Based Classification of Vegetation at Stordalen Mire near Abisko by using High-Resolution Aerial Imagery

324 Marit Aalrust Ripel (2014) Natural hazards and farmers experience of climate change on highly populated Mount Elgon, Uganda

325 Benjamin Kayatz (2014) Modelling of nitrous oxide emissions from clover grass ley – wheat crop rotations in central eastern Germany - An application of DNDC

326 Maxime Rwaka (2014) An attempt to investigate the impact of 1994 Tutsi Genocide in Rwanda on Landscape using Remote Sensing and GIS analysis

327 Ruibin Xu (2014) Spatial analysis for the distribution of cells in tissue sections

328 Annabelle Finck (2014) Bird biodiversity in relation to forest composition in Sweden

329 Tetiana Svystun (2015) Modeling the potential impact of climate change on the distribution of Western Corn Rootworm in Europe